Coupling Gd-DTPA with a bispecific, recombinant protein anti-EGFR-iRGD complex improves tumor targeting in MRI

XIAOYAN XIN[1*], HUIZI SHA[2*], JINGTAO SHEN[3], BING ZHANG[1], BIN ZHU[1] and BAORUI LIU[2]

[1]Department of Radiology, Affiliated Drum-Tower Hospital of Nanjing University Medical School; [2]The Comprehensive Cancer Center of Drum-Tower Hospital, Medical School of Nanjing University and Clinical Cancer Institute of Nanjing University; [3]Department of Nuclear Medicine, Affiliated Drum-Tower Hospital of Nanjing University Medical School, Nanjing 210008, P.R. China

Received November 23, 2015; Accepted March 29, 2016

DOI: 10.3892/or.2016.4712

Abstract. Recombinant anti-epidermal growth factor receptor-internalizing arginine-glycine-aspartic acid (anti-EGFR single-domain antibody fused with iRGD peptide) protein efficiently targets the EGFR extracellular domain and integrin αvβ/β5, and shows a high penetration into cells. Thus, this protein may improve penetration of conjugated drugs into the deep zone of gastric cancer multicellular 3D spheroids. In the present study, a novel tumor-targeting contrast agent for magnetic resonance imaging (MRI) was developed, by coupling gadolinium-diethylene triamine pentaacetate (Gd-DTPA) with the bispecific recombinant anti-EGFR-iRGD protein. The anti-EGFR-iRGD protein was extracted from *Escherichia coli* and Gd was loaded onto the recombinant protein by chelation using DTPA anhydride. Single-targeting agent anti-EGFR-DTPA-Gd, which served as the control, was also prepared. The results of the present study showed that anti-EGFR-iRGD-DTPA-Gd exhibited no significant cytotoxicity to human gastric carcinoma cells (BGC-823) under the experimental conditions used. Compared with a conventional contrast agent (Magnevist), anti-EGFR-iRGD-DTPA-Gd showed higher T1 relaxivity (10.157/mM/sec at 3T) and better tumor-targeting ability. In addition, the signal intensity and the area under curve for the enhanced signal time in tumor, *in vivo*, were stronger than Gd-DTPA alone or the anti-EGFR-Gd control. Thus, Gd-labelled anti-EGFR-iRGD has potential as a tumor-targeting contrast agent for improved MRI.

Correspondence to: Dr Baorui Liu, The Comprehensive Cancer Center of Drum-Tower Hospital, Medical School of Nanjing University and Clinical Cancer Institute of Nanjing University, 321 Zhongshan Road, Nanjing 210008, P.R. China
E-mail: baoruiliu@nju.edu.cn

*Contributed equally

Key words: gadolinium, magnetic resonance imaging, tumor targeting, bispecific recombinant protein, contrast agent

Introduction

Magnetic resonance imaging (MRI) is an important tool used in the diagnosis of cancer (1). To improve the specificity and sensitivity of MRI, contrast agents are used to increase the signal intensity. Numerous different metallic contrast agents, based on gadolinium (Gd) (Magnevist, ProHance), Fe (Feridex, Endorem), and Mn (Teslascan), are currently available (2). Of these, paramagnetic contrast agents based on Gd are better for tumor and vascular imaging, and Gd-diethylene triamine pentaacetate (Gd-DTPA, Magnevist) is the most commonly used MRI contrast agent. However, due to their low molecular weights, conventional MRI contrast agents have short imaging lifetime *in vivo* and lack specificity for target organs. To overcome these drawbacks, nanoparticles were proposed to be ideal as molecular probes and as MRI contrast agents, and generally were able to overcome the drawbacks of small molecule agents. Thus, some nanoparticles have been developed for molecular imaging (3).

Besides nanoparticles, single-domain antibodies (referred to as nanobodies) have attracted much interest for molecular imaging investigations, using modalities such as radionuclide-based, optical, and ultrasound imaging (4-8). Nanobodies have many advantages owing to their small molecular size, and can rapidly be distributed in the bloodstream and easily reach target tissues within a short period of time following injection, exhibiting great potential for tumor detection (9). Nanobodies bind tightly to targets on the surfaces of cancer cells and can be internalized. Nanobodies also have a low immunogenic potential and are rapidly cleared when unbound, allowing for the acquisition of images with a high tumor-to-background contrast at early time points after their administration. They are also stable and specific (9).

Targeting tumors with nanobodies for cancer imaging and therapy has emerged as a promising diagnostic and therapeutic approach. Since epidermal growth factor receptor (EGFR) is highly expressed in a variety of tumors, targeting with a contrast agent using anti-EGFR nanobody has potential advantages. Single-photon emission computed tomography (SPECT) imaging of EGFR expression using an anti-EGFR nanobody as the targeting agent was first reported by Huang *et al* (10). The radiolabelled nanobody demonstrated

high specificity and selectivity towards EGFR-expressing cells. Vosjan *et al* (4,11) reported positron emission tomography (PET) imaging of EGFR expression using the 7D12 nanobody. Biodistribution studies (11) revealed high tumor uptake of these nanobodies in EGFR-positive tumors and a high tumor-to-blood ratio within 1 h post-injection.

The arginine-glycine-aspartic acid (RGD) peptide has been used for tumor penetration in previous studies investigating molecular imaging agents for tumors (5-8). These peptides are known to have a relatively high and specific affinity for the αvβ3-integrin receptor, which is highly expressed in tumor vascular endothelial cells during angiogenesis in various tumor types. Internalizing RGD (iRGD with a sequence of CRGDKGPDC) differs from the RGD peptide in that it is tumor-specific, is composed of nine amino acid residues, and has high cell permeability. iRGD can target αvβ3-integrin receptor and neuropilin-1 (NRP-1), which are highly expressed in a wide variety of tumor cells (12-14). iRGD conjugated with radiolabels such as ^{125}I or ^{18}F has been used to image αvβ3-integrin receptor and NRP-1 expression using nuclear imaging methods including SPECT and PET. This approach of nuclear imaging with radiolabelled iRGD peptides has been shown to be effective and sensitive (15,16).

In the present study, a previously described recombinant protein with dual specificity and high permeability, anti-EGFR-iRGD, was used. Recombinant anti-EGFR-iRGD protein targeted the EGFR extracellular domain and integrin αvβ3/β5, had a high penetration, and improved penetration of other drugs into the deep zone of gastric cancer 3D multicellular spheroids (17).

Although nanobodies have shown potential as molecular imaging contrast agents in several imaging techniques, such as SPECT, PET, optical imaging, and ultrasound, the limited spatial resolution of these imaging techniques prevents ascertaining the exact location of the tumor. Compared with the above methods, MRI has a better spatial resolution and can obtain precise anatomical localization. Absence of radioactivity is another important advantage. However, loading the fusion protein with Gd to construct a targeting contrast agent for MRI is challenging. Gd-chelates may be encapsulated inside a nanoparticle core, absorbed on the surface, or covalently bound (18). However, the relaxivity of Gd-loaded material for encapsulation and release/ leakage of free Gd from the Gd-nanoparticle complex was another clinical concern. Therefore, chemical conjugation may be the most effective method to load Gd with the targeting recombinant protein.

In the present study, we examined a reliable method to construct a bispecific MRI contrast agent with high permeability.

Materials and methods

Materials. Gd-DTPA (Magnevist) was purchased from Bayer Schering Pharma AG (Berlin, Germany). 3-(4,5-dimethylthiazol-2-yl)-2,5-diphenyltetrazolium bromide (MTT) for the cell viability assays and DTPA and $GdCl_3 \cdot 6H_2O$ were obtained from Sigma-Aldrich (St. Louis, MO, USA). All other reagents and solvents of analytical grade were obtained from different commercial sources. Human gastric adenocarcinoma cells (BGC-823) were purchased from the Cell Bank of Shanghai Institute of Biochemistry and Cell Biology (Shanghai, China) and cultured in RPMI-1640 medium supplemented with 10% foetal calf serum, 100 U/ml penicillin, and 100 μg/ml streptomycin, and incubated at 37˚C and 5% CO_2.

Synthesis and characterization of anti-EGFR-DTPA-Gd and anti-EGFR-iRGD-DTPA-Gd. Recombinant proteins anti-EGFR and anti-EGFR-iRGD were prepared as reported previously (16). The synthesis of anti-EGFR-iRGD-DTPA-Gd is shown in Fig. 1. DTPA anhydride (DTPAA) was synthesized as previously reported (19). The fusion proteins and DTPAA (2:1, mol/mol) were added gradually to $NaHCO_3$ solution (0.1 M, pH 9) and stirred for 24 h at room temperature. The reaction mixture was then dialyzed against water [molecular weight cut-off (MWCO) 3500] for 24 h, during which time the water was changed every 3 h, and the purified anti-EGFR-DTPA and anti-EGFR-iRGD-DTPA were obtained. The anti-EGFR-DTPA or anti-EGFR-iRGD-DTPA and $GdCl_3 \cdot 6H_2O$ were mixed in an Eppendorf tube (Thermo Fisher Scientific, Waltham, MA, USA) at a molar ratio of 1:1, and the pH of the solution was adjusted to 7.0. The resulting mixture was agitated for 24 h at 60˚C. The reaction liquid was dialyzed (MWCO 3500) for 24 h, and the water was changed every 3 h. The purified anti-EGFR-DTPA-Gd and anti-EGFR-iRGD-DTPA-Gd were lyophilized to a powder and stored for subsequent use. Gd content of the formed anti-EGFR-DTPA-Gd and anti-EGFR-iRGD-DTPA-Gd were determined by inductively coupled plasma-optical emission spectroscopy (ICP-OES).

In vitro cytotoxicity of anti-EGFR-DTPA-Gd and anti-EGFR-iRGD-DTPA-Gd. Cell viability was determined using the MTT assay. Briefly, BGC-823 cells in the logarithmic phase were seeded at 70-80% confluence per well in 96-well plates, incubated at 37˚C overnight, and treated with the indicated concentrations of anti-EGFR-DTPA-Gd and anti-EGFR-iRGD-DTPA-Gd, or DTPA-Gd for 48 h. Following treatment, 10 μl of 5 mg/ml MTT was added, and the cells were incubated for 4 h at 37˚C. The supernatant was discarded, and 100 μl of dimethylsulphoxide (DMSO) was added to each well. The absorbance in each well was measured by a Multiskan Spectrum Microplate Reader (Thermo Fisher Scientific, Waltham, MA, USA) at 570 and 630 nm, and the net A570-A630 was taken as the index of cell viability. The net absorbance from the wells of the cells cultured with complete medium was taken as 100% viability. The viability of the treated cells was calculated using the formula: % viability = $(A_{570}-A_{630})$ treated/$(A_{570}-A_{630})$ control x 100%.

In vitro cell targeting and competitive binding assay. To examine whether anti-EGFR-DTPA-Gd and anti-EGFR-iRGD-DTPA-Gd targeted BGC-823 cells, anti-EGFR-DTPA-Gd or anti-EGFR-iRGD-DTPA-Gd were labelled with fluorescein isothiocyanate (FITC). Briefly, purified proteins were suspended at a concentration of 1 mg/ml, in conjugation buffer (National Medicine Company, Shanghai, China) (7.56 g $NaHCO_3$, 1.06 g Na_2CO_3, 7.36 g NaCl, in 1 l) at 4˚C and the pH was adjusted to 9.0. Freshly prepared FITC (1 mg/ml in

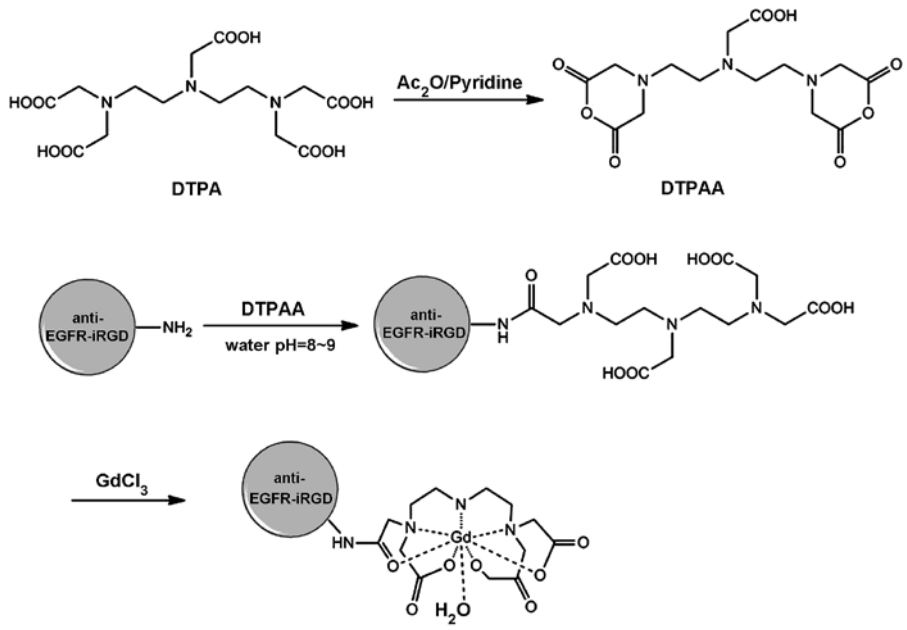

Figure 1. Synthetic route of anti-epidermal growth factor receptor-internalizing arginine-glycine-aspartic acid-diethylene triamine pentaacetate-gadolinium (anti-EGFR-iRGD-DTPA-Gd).

DMSO) was added to the antibody solution (at protein: FITC ratio of 1 mg:150 μg) gradually, agitating while adding to ensure proper mixing and the solution was left at 4˚C for conjugation reaction for 8 h in the dark. NH_4Cl was added to a final concentration of 50 mM to terminate the reaction at 4˚C. The conjugate was then dialyzed against phosphate-buffered saline (PBS) until the dialysate was clear.

BGC-823 cells in the logarithmic phase were seeded in 24-well chamber slides at 50% confluence per well. After 16 h, PBS supplemented with 5% bovine serum albumin was added to the wells for blocking and incubated at 37˚C with the appropriate FITC-labelled anti-EGFR-DTPA-Gd or anti-EGFR-iRGD-DTPA-Gd for 1 h. The cells were washed three times with cold PBS (pH 7.4), the nucleus was labelled with Hoechst 33258, and the fixed cells were observed with a fluorescence microscope (Zeiss LSM710, Carl Zeiss, Germany). Competitive binding assays were performed. Briefly, BGC-823 cells in the logarithmic phase were treated as described above and incubated with anti-EGFR-DTPA-Gd-FITC or anti-EGFR-iRGD-DTPA-Gd-FITC and an appropriate concentration of competing EGFR rabbit monoclonal antibody (dilution, 1:500; cat. no. 1114-1) (cetuximab or iRGD) at 37˚C for 1 h. The cells were washed in PBS and fixed, and the nucleus was stained with Hoechst 33258. The cells were then observed under a fluorescent microscope.

MRI in vitro. *In vitro* MRI was performed on a 3.0 Tesla Achieve scanner (Philips Medical Systems, Best, The Netherlands). The T1-weighted MR images and T1-map images of anti-EGFR-iRGD-DTPA-Gd and Gd-DTPA injections were obtained. MR images were captured at different concentrations of Gd (77, 38.4, 19.2, 9.6, 4.8 and 2.4 μM). The samples were tested using T1-weighted and T1-map pulse sequences. T1-weighted pulse sequences held the time of echo constant at 15 msec while varying the time of repetition to 200, 400, 700, 900, 1,200, 1,500, 2,000, 2,500 and 3,500 msec, respectively. Quantitative T1 relaxation maps were reconstructed from the datasets. The T1 value of the samples was measured for each of the contrast agents.

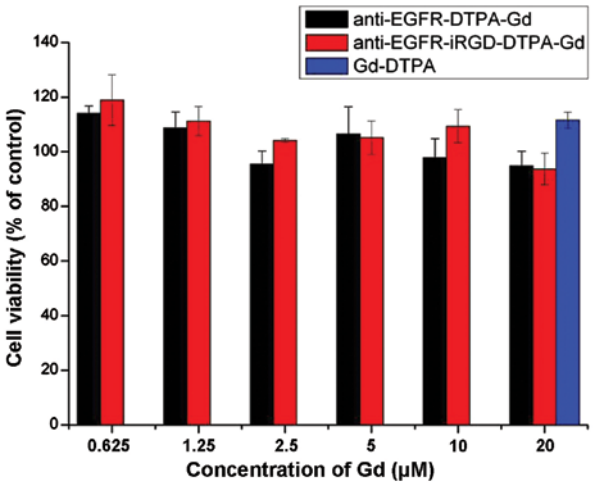

Figure 2. Cytotoxicity of the anti-epidermal growth factor receptor-diethylene triamine pentaacetate-gadolinium (anti-EGFR-DTPA-Gd) and anti-EGFR-internalizing arginine-glycine-aspartic acid (iRGD)-DTPA-Gd in BGC-823 tumor cell lines. Anti-EGFR-DTPA-Gd and anti-EGFR-iRGD-DTPA-Gd at various concentrations were added to the BGC-823 cell suspensions and incubated for 48 h. Cell viability was measured using an MTT assay.

Evaluation of the targeting in vivo: MRI in nude mouse tumor model. Animal procedures were carried out in compliance with guidelines set by the Animal Care Committee at Drum Tower Hospital (Nanjing, China). To prepare the xenograft mouse model, athymic nude BALB/c mice (5-6 weeks, male; weighing, 18-22 g) were purchased from Shanghai SLAC Laboratory Animal Co., Ltd. (Shanghai, China). BGC-823

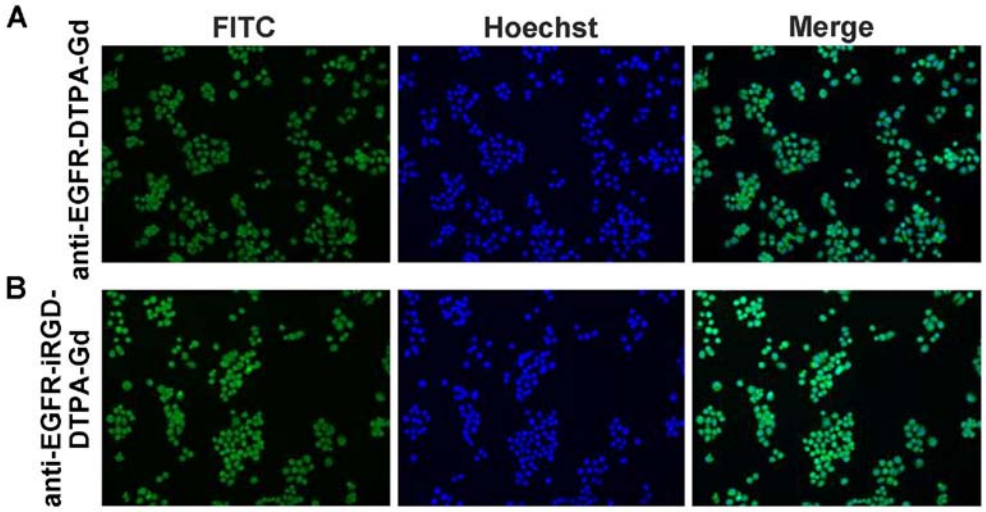

Figure 3. The uptake of BGC-823 cells with fluorescein isothiocyanate (FITC)-labeled (A) anti-epidermal growth factor receptor-diethylene triamine pentaacetate-gadolinium (anti-EGFR-DTPA-Gd) and (B) anti-EGFR-internalizing arginine-glycine-aspartic acid (iRGD)-DTPA-Gd was analyzed. BGC-823 cells were incubated with a sub-saturating concentration of (A) anti-EGFR-DTPA-Gd and (B) anti-EGFR-iRGD-DTPA-Gd. Nuclei were stained with Hoechst 33258. Fuorescence images are shown (magnification, x200).

cells were collected by trypsin digestion, and five million cells in 0.1 ml serum-free culture medium were injected into the right axilla of each mouse on day 0. When the tumor volume increased to 400 mm^3 (approximately day 15), MRI was performed on the mice. Tumor volumes were calculated from two diameter measurements using a digital vernier calliper and the formula: tumor volume = (length x $width^2$)/2, where length is the longest dimension and width is the widest dimension.

MRI was performed using a 3.0T MR scanner (Achieve 3.0T, Philips Medical Systems). Tumor-bearing mice were randomly divided into the anti-EGFR-iRGD-DTPA-Gd (n=5), anti-EGFR-DTPA-Gd (n=5), and pure Gd-DTPA for MRI (n=5) groups. The mice were anesthetized by intraperitoneal injection of a mixture of ketamine and xylazine. After anaesthesia, the tumor-bearing mice were placed in a home-built cradle (22-26˚C, relative humidity: 40-70%, food: 5 g/100 g and water: 6-7 ml/100 g). To collect baseline data, the mice were scanned by a T2-weighted image and then scanned by T1-weighted spin-echo sequence. Subsequently, the mice were injected with the indicated paramagnetic contrast agents through tail vein. T1 dynamic scans were taken at 15, 30 min, 1, 2 and 3 h after injection using the same parameters as for pre-contrast imaging. The signal intensity was measured on the contrasted T1-weighted image. The mean areas under the curve (AUC) of the anti-EGFR-iRGD-DTPA-Gd, anti-EGFR-DTPA-Gd, and DTPA-Gd groups of different organs were calculated by the trapezoidal method [$AUC_{(0-t)}$].

Statistical analysis. Data are presented as the mean ± standard deviation. Statistical tests were performed using SPSS 15.0 (SPSS, Inc., Chicago, IL, USA). Unpaired Student's t-tests were used to compare the means of 2 groups. For multiple comparisons between groups, a one-way ANOVA was performed to detect statistical differences. Differences within the ANOVA were determined using a Tukey's post hoc test. $P<0.05$ was considered to indicate a statistically significant difference.

Results

Synthesis and characterization. Recombinant proteins anti-EGFR and anti-EGFR-iRGD were purified successfully as reported previously (16). The synthesis of anti-EGFR-iRGD-DTPA-Gd is shown in Fig. 1. The Gd concentration of the Gd-conjugated anti-EGFR-iRGD was 78 μM, as determined by ICP-OES. According to the pre-experiment, the protein and Gd were determined at a ratio of 1:2 to obtain optimal reaction conditions.

In vitro cytotoxicity of anti-EGFR-DTPA-Gd and anti-EGFR-iRGD-DTPA-Gd. *In vitro* toxicity of anti-EGFR-DTPA-Gd and anti-EGFR-iRGD-DTPA-Gd, and Gd-DTPA at different indicated molar concentrations of Gd was evaluated using the MTT assay in BGC 823 cells. Magnevist at 20 μM was taken as the positive control. As shown in Fig. 2, the cell survival rates at different concentrations of the anti-EGFR-DTPA-Gd and anti-EGFR-iRGD-DTPA-Gd were not significantly different ($P>0.05$). Compared with the Magnevist group, the cell survival rates for the anti-EGFR-DTPA-Gd- and anti-EGFR-iRGD-DTPA-Gd-treated groups were slightly lower, although the differences were not significant ($P>0.05$). The cell survival rates of all the groups were >90%, suggesting that anti-EGFR-DTPA-Gd and anti-EGFR-iRGD-DTPA-Gd did not influence the viability of BGC823 cells at the concentrations used in the present study.

In vitro cell targeting and competitive binding assay. BGC-823 cells incubated with anti-EGFR-DTPA-Gd-FITC or anti-EGFR-iRGD-DTPA-Gd-FITC, exhibited green fluorescence. Thus, anti-EGFR-DTPA-Gd-FITC and anti-EGFR-iRGD-DTPA-Gd-FITC were able to target gastric cancer BGC-823 cells (Fig. 3). When cetuximab (a monoclonal anti-EGFR antibody acting as an inhibitor) or iRGD were added, the uptake of anti-EGFR-DTPA-Gd-FITC and anti-EGFR-iRGD-DTPA-Gd-FITC in BGC-823 cells decreased as proven by the decreased fluorescent emission (Fig. 4).

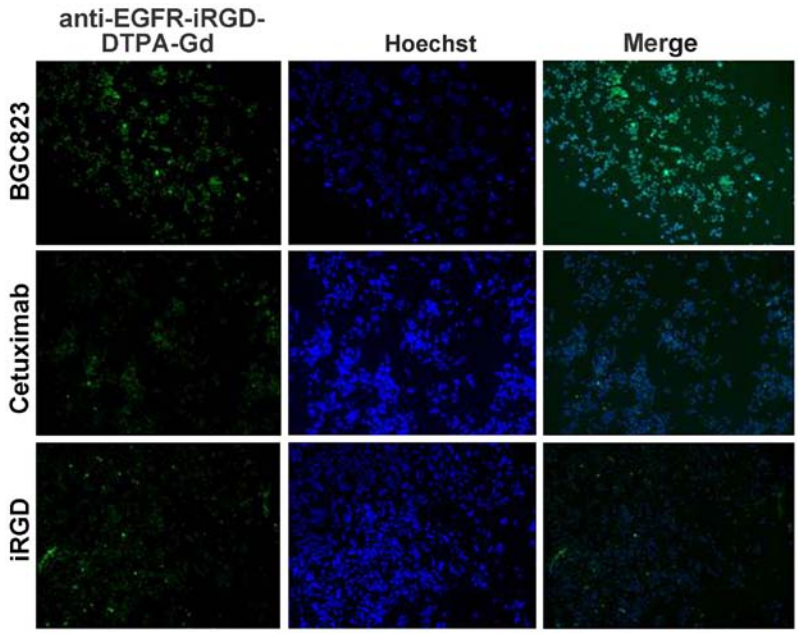

Figure 4. The competition and binding profile of BGC-823 cells with fluorescein isothiocyanate (FITC)-labeled anti-epidermal growth factor receptor-internalizing arginine-glycine-aspartic acid-diethylene triamine pentaacetate-gadolinium (anti-EGFR-iRGD-DTPA-Gd) was analyzed. The analyses of BGC-823 tumor cells by competitive binding assay are shown according to FITC-labeled anti-EGFR-iRGD-DTPA-Gd. BGC-823 cells were incubated with a sub-saturating concentration of anti-EGFR-iRGD-DTPA-Gd-FITC and an indicated concentration of competing mAb cetuximab or iRGD. The fluorescence images are shown (magnification, x100).

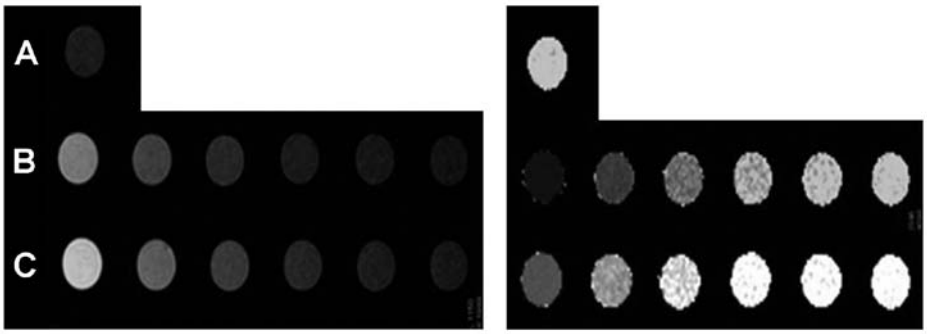

Figure 5. T1-weighted images (left) and T1-map images (right) of different gadolinium (Gd) concentration of anti-epidermal growth factor receptor-internalizing arginine-glycine-aspartic acid-diethylene triamine pentaacetate-Gd (anti-EGFR-iRGD-DTPA-Gd) and Gd-DTPA. The concentration of Gd was 77, 38.4, 19.2 9.6, 4.8 and 2.4 μM, respectively. (A) Saline, (B) anti-EGFR-iRGD-DTPA-Gd and (C) DTPA-Gd.

As shown in Fig. 3, the fluorescence intensity of anti-EGFR-iRGD-DTPA-Gd was stronger after being mixed with 25 μg/ml cetuximab or 10 μg/ml iRGD. This finding indicated that anti-EGFR-iRGD-DTPA-Gd binds the same receptor as cetuximab and iRGD. The specificity and affinity of anti-EGFR-iRGD-Gd binding to the target antigen were assessed using a competitive binding assay. When fluorescence intensity for anti-EGFR-iRGD-Gd-FITC taken up by BGC-823 was set as 100%, the affinity of anti-EGFR-iRGD-Gd was decreased to 20.9 or 41.3% when cetuximab or iRGD was added to compete with the antigen (Fig. 4). These results are semiquantitative as calculated by the microscopy software. The binding of anti-EGFR-iRGD-Gd to BGC-823 cells was specifically inhibited by cetuximab and iRGD, indicating that anti-EGFR-iRGD-Gd binds to the same receptor. These results indicated that anti-EGFR-iRGD-Gd possesses specificity and affinity to EGFR and was internalized through the same route as iRGD.

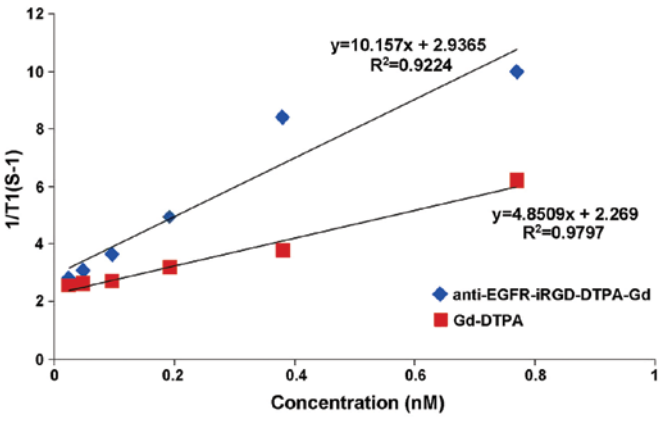

Figure 6. Relaxivity of anti-epidermal growth factor receptor-internalizing arginine-glycine-aspartic acid-diethylene triamine pentaacetate-gadolinium (anti-EGFR-iRGD-DTPA-Gd) and Gd-DTPA. The relaxivity of anti-EGFR-iRGD-DTPA-Gd and Gd-DTPA were calculated by Gd concentration and T1 value.

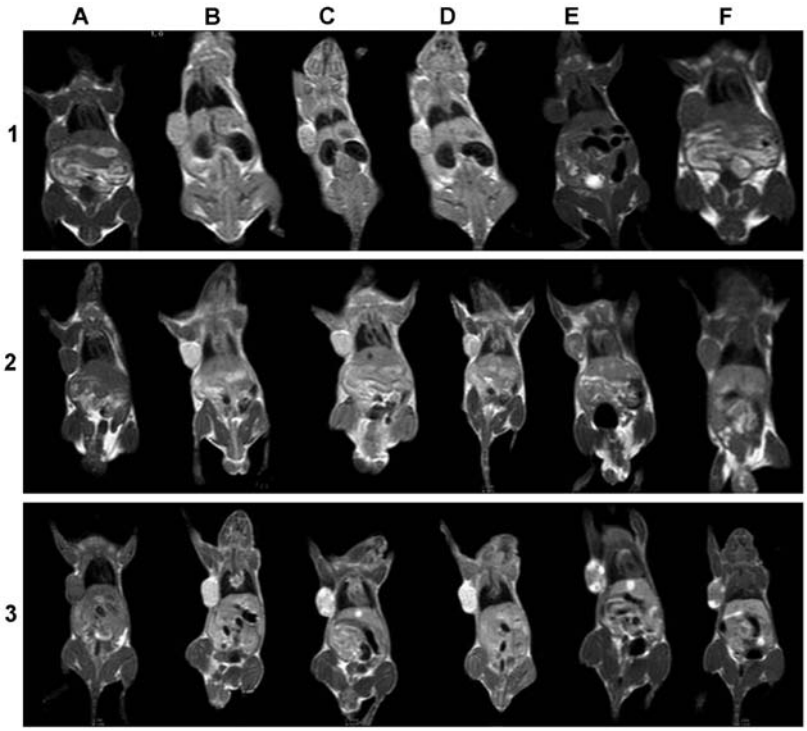

Figure 7. MRI of BGC-823 tumor-bearing mice. Mice received 1) gadolinium-diethylene triamine pentaacetate (Gd-DTPA), 2) anti-epidermal growth factor receptor (EGFR)-DTPA-Gd, or 3) anti-EGFR-internalizing arginine-glycine-aspartic acid (iRGD)-DTPA-Gd injections via the tail vein at different time points. (A) Precontrast, (B) 15 min, (C) 30 min, (D) 1 h, (E) 2 h, and (F) 3 h.

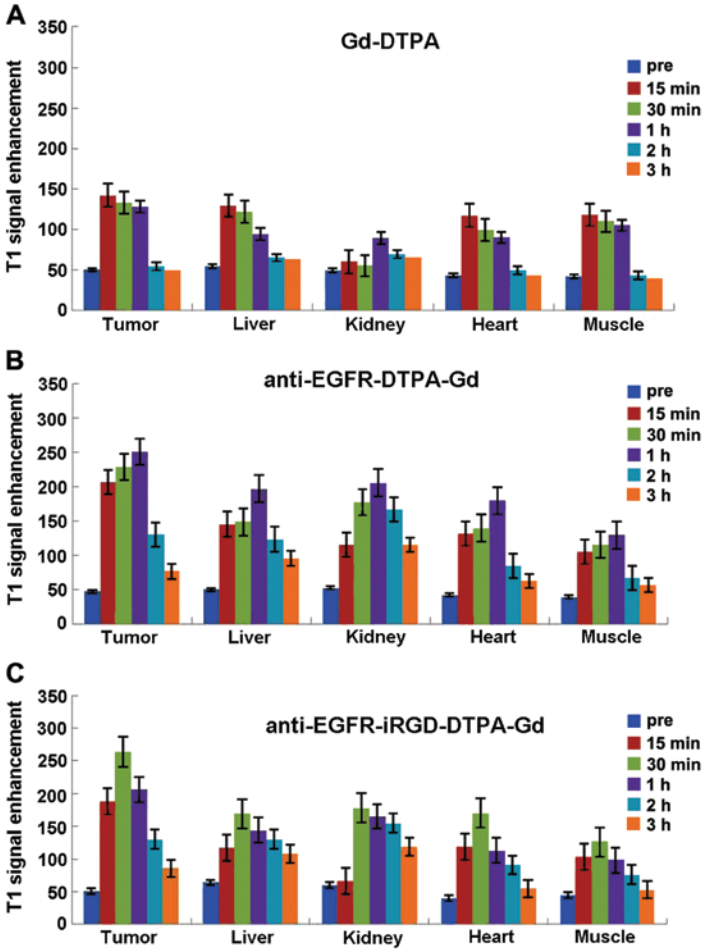

Figure 8. Results of the enhanced signals in different tissues *in vivo*. (A) Gadolinium-diethylene triamine pentaacetate (Gd-DTPA), (B) anti-epidermal growth factor receptor (EGFR)-DTPA-Gd, and (C) anti-EGFR-internalizing arginine-glycine-aspartic acid (iRGD)-DTPA-Gd.

MRI in vitro. To test the ability of anti-EGFR-iRGD-DTPA-Gd as a MRI contrast agent, the T1 longitudinal relaxation time of H_2O protons was evaluated. H_2O, anti-EGFR-DTPA-Gd, anti-EGFR-iRGD-DTPA-Gd, and Gd-DTPA injections [(Gd)=2.4-77 μM] were evaluated at 3.0T at 24˚C. As shown in Fig. 5, in the anti-EGFR-iRGD-DTPA-Gd group, higher Gd concentrations showed higher signal intensities in the T1-weighted image and shorter T1 values in the T1-map image. The anti-EGFR-iRGD-DTPA-Gd group showed a higher signal intensity in the T1-weighted image and a shorter T1 value in the T1-map image than those of the Gd-DTPA group at the same Gd concentrations (P<0.05). The relaxivity 'r' was defined as the slope of the curves 1/T1 with respect to the contrast agent Gd concentration. The 'r' of anti-EGFR-iRGD-Gd was 10.157/mM/sec and higher than Gd-DTPA (4.851/mM/sec) (Fig. 6). The results of the MRI *in vitro* indicated that anti-EGFR-iRGD-DTPA-Gd is a better and novel MRI molecular contrast agent, when compared with DTPA-Gd.

Evaluation of the targeting in vivo: MRI in nude mouse tumor model. For MRI, anti-EGFR-iRGD-DTPA-Gd, anti-EGFR-DTPA-Gd, and Gd-DTPA were injected into tumor-bearing mice via the vena caudalis at 42 μmol Gd/kg. The mice were scanned at 15, 30 min, 1, 2 and 3 h following contrast injection. MRI and the results of the enhanced signals in different tissues are summarized in Figs. 7 and 8.

As shown in Figs. 7-1 and 8A, prior to the injection of Gd-DTPA, the images of tumors and other organs were dark (Fig. 7A). After the administration of Magnevist, the contrast agents were non-specifically distributed throughout the body in a short period of time. The signal-to-noise tumor ratio increased from 33 to 50 by 15 min after injection of Gd-DTPA. Liver of this group also brightened and the signal-to-noise ratio reached a maximum (from 36 to 46) by 15 min after injection and then rapidly decayed (Fig. 7-1B and C). Since the elimination of Gd-DTPA was by renal clearance, an enhancement in the kidney continued from 15 min to 1 h (from 32 to 42) (Fig. 7-1D), and the urinary bladder became extremely bright compared to other tissues by 1 h after injection of Gd-DTPA (Fig. 7-1E). The heart and muscle also reached a maximum at 15 min after injection that was then followed by a rapid decay. The entire body was as dark as preinjection by 2 h after injection of Gd-DTPA (Fig. 7-1F).

After the injection of anti-EGFR-DTPA-Gd, the contrast in the tumor was well distributed and the tumor was significantly bright, with its boundary clearly distinct (Fig. 7-2). The signal-to-noise ratio of the tumor increased significantly from 31 to 67 by 15 min and reached a maximum at 1 h (from 31 to 100) (Fig. 8C). The liver and kidney were also enhanced and the signal intensity signal-to-noise ratio reached a maximum (from -33 to -82 and from 34 to -111, respectively) by 1 h after the injection, followed by rapid decay (Fig. 7-2D). Similar to the above result, the signal intensities of the heart and muscle were enhanced to a maximum by 1 h after injection and then gradually decreased. After 3 h, the enhanced signal intensity was barely detectable.

After the injection of anti-EGFR-iRGD-DTPA-Gd, the tumor signal was brighter than that of other tissues, and the boundary was also clearly distinct (Fig. 7-3). The signal-to-noise ratio of the tumor was maximal 30 min after injection (from -34 to -98) and then gradually decreased (Fig. 8C). After 3 h, an enhanced signal was present at the tumor margins. The signal-to-noise ratio of the liver and kidney was also maximal at 30 min after injection (from -42 to 87 and from 40 to -89, respectively) and decreased gradually. The signal intensity of heart and muscle was maximal at 30 min after injection and then decreased gradually. After 3 h, the enhanced signal intensity remained higher than preinjection.

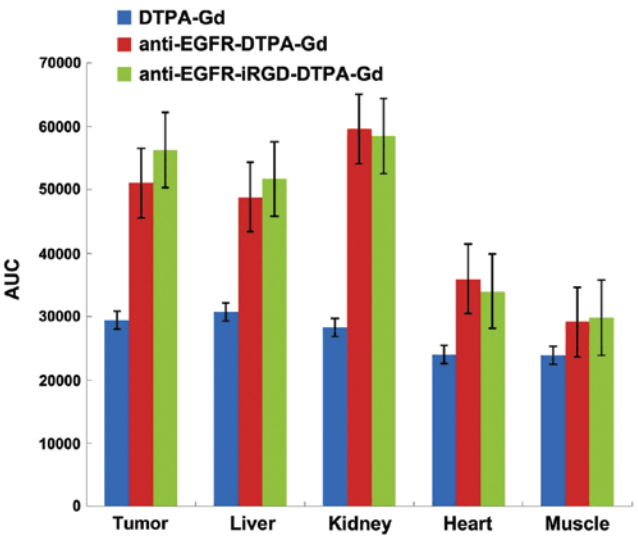

Figure 9. The area under the enhanced signal-time curve (AUC) of gadolinium-diethylene triamine pentaacetate (Gd-DTPA), anti-epidermal growth factor receptor (EGFR)-DTPA-Gd, and anti-EGFR-internalizing arginine-glycine-aspartic acid (iRGD)-DTPA-Gd in different tissues.

The enhanced AUCs of anti-EGFR-iRGD-DTPA-Gd, anti-EGFR-DTPA-Gd, and Magnevist were calculated by the trapezoidal method. The results are shown in Fig. 9. Compared to Gd-DTPA and anti-EGFR-DTPA-Gd, anti-EGFR-iRGD-DTPA-Gd exhibited significant target enhancements in the tumor and liver (P<0.01). In kidney, heart, and muscle, anti-EGFR-DTPA-Gd had greater enhancements than anti-EGFR-iRGD-DTPA-Gd and Gd-DTPA (P<0.01).

Discussion

In the present study, we designed and synthesized a novel tumor-targeted molecular MRI contrast agent, which was constructed by the conjugation of Gd-DTPA to a bispecific recombinant protein of high permeability anti-EGFR-iRGD. This novel agent has no cytotoxicity, and anti-EGFR-iRGD-DTPA-Gd was capable of targeting the same receptor as cetuximab and iRGD *in vitro*. Furthermore, *in vivo* MR images showed that signal enhancements in tumors after injection of anti-EGFR-iRGD-DTPA-Gd were significantly higher than those of anti-EGFR-DTPA-Gd or pure Gd-DTPA.

Uppal *et al* reported that targeting with Gd^{3+} probe mainly includes three types (20): i) discrete targeting peptide-Gd-chelate: use of smaller molecules in combination with one or more of the Gd chelate; ii) self-assembled nanoparticles including Gd, which are usually emulsions, microcapsule or liposome nanoparticles containing 10-1,000 Gd chelates

prepared by self-assembly method; and iii) 'smart' probes with triggering activity, the product after biochemical reactions (such as enzyme pyrolysis reaction and pH change) between probes and target material can improve the effect of relaxivity. The synthetic probe in this experiment belongs to the first category. Its advantage lies in the small size of probes. The probe can freely pass through the endothelial cell barrier into the imaging target and produce higher target-background signal.

N-terminal cysteine containing tumor-homing peptide (iRGD, CRGDK/EGPD/EC) has been identified as a highly efficient, deep penetrating peptide (21,22). When iRGD is chemically conjugated to or co-administered with an anticancer drug, this peptide can carry the drug deep into extravascular tumor tissue. iRGD also homes to tumors in a tumor-specific and NRP-1-dependent manner. Thus, when the polymer nanoparticles are modified or co-administered with iRGD, the tissue penetrating and targeting abilities of drug-loaded nanoparticles may be improved. In the present study, anti-EGFR-iRGD fusion protein was confirmed to maintain the tumor tissue-targeting abilities, which is consistent with previous results (17).

For the *in vivo* MRI study, a human gastric cancer xenograft model with BGC-823 cells was established. The images on the 3.0T MR scanner showed that the tumor was enhanced clearly by Gd-DTPA, anti-EGFR-DTPA-Gd and anti-EGFR-iRGD-DTPA-Gd. However, analysis of the MRI signal intensity revealed different time-dependent enhancement patterns for the three groups. In the pure Gd-DTPA group, the tumor signal intensity reached a maximum more rapidly with mild enhancement and showed a rapid clearance because the molecular weight of Gd-DTPA is small (~500 Da) and the water-soluble Gd chelates diffuse from the tumor tissue easily. In the anti-EGFR-DTPA-Gd group, the signal intensity of the tumor reached a maximum at 1 h (from 47 to 221) and the signal intensity of the tumor was higher than that of pure Gd-DTPA. We suggest that the enhancement of anti-EGFR-DTPA-Gd is caused by the specific binding to endothelial and tumor cells. In comparison to anti-EGFR-DTPA-Gd, the signal intensity of the tumor of anti-EGFR-iRGD-DTPA-Gd reached a maximum at 30 min (from 51 to 264) and the signal intensity of tumor was higher than that of anti-EGFR-DTPA-Gd. EGFR is overexpressed in BGC-823 cells, and anti-EGFR-iRGD-DTPA-Gd can target tumor cells and be restricted to the tumor area by the tumor cell surface EGFR-antibody reaction. On the other hand, iRGD increased the penetration of anti-EGFR-iRGD-DTPA-Gd. In addition, anti-EGFR-iRGD-Gd has a large magnetic moment due to the covalent linkage of Gd-DTPA to anti-EGFR-iRGD, and a larger molecular weight. We hypothesize that the use of iRGD increases the penetrance of the contrast agent to the cells and therefore, shortens the time required for reaching the maximum signal.

In conclusion, a novel tumor-targeting molecular MRI contrast agent was designed and synthesized, which was constructed by the conjugation of Gd-DTPA to a bispecific recombinant protein with high permeability. This novel agent without cytotoxicity targeted gastric cancer cells and shows promise as an effective novel MRI molecular contrast agent and for early diagnostic imaging in clinical applications.

Acknowledgements

The present study was supported by the Science and Technology Development fund of Nanjing (no. YKK12065), Health Research projects in Jiangsu Province (no. Q201411), the National Natural Science Foundation of China (no. 81502037), Fundamental Research Funds for the Central Universities (no. 20610140698), and the Scientific Research Foundation of the Graduate School of Nanjing University (no. 2013CL15).

References

1. Weissleder R: Molecular imaging in cancer. Science 312: 1168-1171, 2006.
2. Hu F, Joshi HM, Dravid VP and Meade TJ: High-performance nanostructured MR contrast probes. Nanoscale 2: 1884-1891, 2010.
3. Moffat BA, Reddy GR, McConville P, Hall DE, Chenevert TL, Kopelman RR, Philbert M, Weissleder R, Rehemtulla A and Ross BD: A novel polyacrylamide magnetic nanoparticle contrast agent for molecular imaging using MRI. Mol Imaging 2: 324-332, 2003.
4. Vosjan MJ, Vercammen J, Kolkman JA, Stigter-van Walsum M, Revets H and van Dongen GA: Nanobodies targeting the hepatocyte growth factor: Potential new drugs for molecular cancer therapy. Mol Cancer Ther 11: 1017-1025, 2012.
5. Garanger E, Boturyn D and Dumy P: Tumor targeting with RGD peptide ligands-design of new molecular conjugates for imaging and therapy of cancers. Anticancer Agents Med Chem 7: 552-558, 2007.
6. Chen X, Liu S, Hou Y, Tohme M, Park R, Bading JR and Conti PS: MicroPET imaging of breast cancer alphav-integrin expression with 64Cu-labeled dimeric RGD peptides. Mol Imaging Biol 6: 350-359, 2004.
7. Chen X, Tohme M, Park R, Hou Y, Bading JR and Conti PS: Micro-PET imaging of alphavbeta3-integrin expression with 18F-labeled dimeric RGD peptide. Mol Imaging 3: 96-104, 2004.
8. Haubner R, Wester HJ, Weber WA, Mang C, Ziegler SI, Goodman SL, Senekowitsch-Schmidtke R, Kessler H and Schwaiger M: Noninvasive imaging of alpha(v)beta3 integrin expression using 18F-labeled RGD-containing glycopeptide and positron emission tomography. Cancer Res 61: 1781-1785, 2001.
9. Oliveira S, Heukers R, Sornkom J, Kok RJ and van Bergen En Henegouwen PM: Targeting tumors with nanobodies for cancer imaging and therapy. J Control Release 172: 607-617, 2013.
10. Huang L, Gainkam LO, Caveliers V, Vanhove C, Keyaerts M, De Baetselier P, Bossuyt A, Revets H and Lahoutte T: SPECT imaging with 99mTc-labeled EGFR-specific nanobody for in vivo monitoring of EGFR expression. Mol Imaging Biol 10: 167-175, 2008.
11. Vosjan MJ, Perk LR, Roovers RC, Visser GW, Stigter-van Walsum M, van Bergen En Henegouwen PM and van Dongen GA: Facile labelling of an anti-epidermal growth factor receptor Nanobody with 68Ga via a novel bifunctional desferal chelate for immuno-PET. Eur J Nucl Med Mol Imaging 38: 753-763, 2011.
12. Haspel N, Zanuy D, Nussinov R, Teesalu T, Ruoslahti E and Aleman C: Binding of a C-end rule peptide to the neuropilin-1 receptor: A molecular modeling approach. Biochemistry 50: 1755-1762, 2011.
13. Sugahara KN, Teesalu T, Karmali PP, Kotamraju VR, Agemy L, Girard OM, Hanahan D, Mattrey RF and Ruoslahti E: Tissue-penetrating delivery of compounds and nanoparticles into tumors. Cancer Cell 16: 510-520, 2009.
14. Hiki S and Kataoka K: Versatile and selective synthesis of 'click chemistry' compatible heterobifunctional poly(ethylene glycol)s possessing azide and alkyne functionalities. Bioconjug Chem 21: 248-254, 2010.
15. Hoang B, Lee H, Reilly RM and Allen C: Noninvasive monitoring of the fate of 111In-labeled block copolymer micelles by high resolution and high sensitivity microSPECT/CT imaging. Mol Pharm 6: 581-592, 2009.

16. Ishihara T, Maeda T, Sakamoto H, Takasaki N, Shigyo M, Ishida T, Kiwada H, Mizushima Y and Mizushima T: Evasion of the accelerated blood clearance phenomenon by coating of nanoparticles with various hydrophilic polymers. Biomacromolecules 11: 2700-2706, 2010.
17. Sha H, Zou Z, Xin K, Bian X, Cai X, Lu W, Chen J, Chen G, Huang L, Blair AM, *et al*: Tumor-penetrating peptide fused EGFR single-domain antibody enhances cancer drug penetration into 3D multicellular spheroids and facilitates effective gastric cancer therapy. J Control Release 200: 188-200, 2014.
18. Kielar F, Tei L, Terreno E and Botta M: Large relaxivity enhancement of paramagnetic lipid nanoparticles by restricting the local motions of the Gd(III) chelates. J Am Chem Soc 132: 7836-7837, 2010.
19. Prudêncio M, Rohovec J, Peters JA, Tocheva E, Boulanger MJ, Murphy ME, Hupkes HJ, Kosters W, Impagliazzo A and Ubbink M: A caged lanthanide complex as a paramagnetic shift agent for protein NMR. Chemistry 10: 3252-3260, 2004.
20. Uppal R and Caravan P: Targeted probes for cardiovascular MRI. Future Med Chem 2: 451-470, 2010.
21. Sugahara KN, Teesalu T, Karmali PP, Kotamraju VR, Agemy L, Greenwald DR and Ruoslahti E: Coadministration of a tumor-penetrating peptide enhances the efficacy of cancer drugs. Science 328: 1031-1035, 2010.
22. Sugahara KN, Braun GB, de Mendoza TH, Kotamraju VR, French RP, Lowy AM, Teesalu T and Ruoslahti E: Tumor-penetrating iRGD peptide inhibits metastasis. Mol Cancer Ther 14: 120-128, 2015.